Role of rare earth oxide particles on the oxidation behaviour of silicon carbide coated 2.5D carbon fibre preforms

Murthy, Tammana S R C; Reeman, Lucas; Zou, Ji; Venkatachalam, Vinu; Baker, Benjamin; Wang, Minshi; Binner, Jon

Open Ceramics 2 (2020) 100018

Contents lists available at ScienceDirect

Open Ceramics

journal homepage: www.editorialmanager.com/oceram

Role of rare earth oxide particles on the oxidation behaviour of silicon carbide coated 2.5D carbon fibre preforms

T.S.R.C. Murthy [a,b,*], Lucas Reeman [a], Ji Zou [a,**], Vinothini Venkatachalam [a], Ben Baker [a], Minshi Wang [a], Jon Binner [a,***]

[a] School of Metallurgy and Materials, University of Birmingham, UK
[b] Materials Group, Bhabha Atomic Research Centre, Mumbai, 400085, India

ARTICLE INFO

Keywords:
Carbon fibres
Silicon carbide coating
Rare earth oxides
Chemical vapour infiltration
Oxidation

ABSTRACT

Silicon carbide (SiC) coated carbon fibre preforms are often reported to offer superior mechanical and oxidation resistance compared to those without such coatings, although the use of SiC is limited by its poor oxidation resistance in the presence of moisture, low oxygen partial pressures and/or temperatures above 1550 °C. In an attempt to overcome these limitations, the doping of a SiC coating with two rare earth (RE) oxides, Y_2O_3 and CeO_2, both separately and in combination has been investigated with a view to improving the oxidation resistance. The coating was deposited using chemical vapour infiltration (CVI) of SiC onto the individual fibres within 2.5D carbon fibre preforms and the subsequent oxidation studies were undertaken in the range 1300–1700 °C with and without the presence of the RE oxide particles and with both continuous and isothermal oxidation behaviour being investigated. SiO_2 growth rates were calculated for all the samples at different temperatures. Immiscible solid RE silicates were formed in the molten silica, which are believed to have enhanced the oxidation resistance by two different mechanisms: i) delays in the active oxidation of SiO_2 by decreasing the evaporation of SiO and ii) enhancing the viscosity of molten SiO_2, which further reduces the diffusivity of oxygen through the glassy phase.

1. Introduction

Carbon fibre preforms are often considered as a potential reinforcement for ultra-high temperature ceramics (UHTCs) with the aim of forming ultra-high temperature ceramic matrix composites (UHTCMCs) that exhibit enhanced toughness and hence improved thermal shock resistance [1]. These materials are being considered for a range of applications including rocket nozzles, heat shields, fission/fusion nuclear components, concentrated solar power receivers and thermal protection systems [1–7]. The rapid expansion of carbon fibres into the commercial aerospace market is a testament to their ability to be readily formed into a wide range of large complex shapes whilst not compromising their excellent strength-to-weight ratio [1,8]. They exhibit many excellent advantages compared to other reinforcing fibres; high specific modulus, specific strength and stiffness, outstanding fatigue properties, a negative coefficient of longitudinal thermal expansion and low coefficient of thermal expansion (CTE). Carbon fibre also has relatively good temperature resistance under vacuum or inert gases but is readily oxidised at ~500 °C in air [1,8]. Various types of carbon fibre preforms, including 2D layered, 2.5D needled and 3D woven are commercially available, among these the 2.5D fibre architectures have been shown to be a good compromise between mechanical performance and cost [1]. All carbon fibres need protecting against oxidation, however, and whilst there is evidence that this can be provided by the oxidation of the UHTC matrix at ultra-high temperatures [1,9], silicon carbide (SiC) coatings are often used to provide a barrier against oxidation for service at lower temperatures, e.g. 1400–1500 °C, and against other forms of chemical attack during processing.

Silicon carbide is a popular coating material due to its refractory nature combined with its ability to form a glassy silica layer in oxidizing

* Corresponding author. School of Metallurgy and Materials, University of Birmingham, UK.
** Corresponding author.
*** Corresponding author.
E-mail addresses: murthi@iitkalumni.org, murthi@barc.gov.in (T.S.R.C. Murthy), zouji1983@aliyun.com (J. Zou), J.Binner@bham.ac.uk (J. Binner).

https://doi.org/10.1016/j.oceram.2020.100018
Received 10 August 2020; Accepted 19 August 2020
Available online 26 August 2020

Table 1
Literature data for selected works on the oxidation behaviour of carbon fibres protected by SiC coatings deposited using different techniques.

Coating method	Oxidation conditions	Mass change	Oxidation mechanisms	Ref
Pack cementation	Isothermal 1500 °C for 58 h.	Specimen mass increased rapidly for first 2 h then stable for the next 41 h. After 58 h weight loss reached 2.1%.	Bubble formation & pores on coating surface due to CO_2 forming at the SiC/SiO_2 interface; indicates SiC layer had not completely become silica	[32]
Two step pack cementation	Isothermal 1500 °C for 310 h.	Overall mass loss of 0.63% after oxidation for 310 h, but 4 regimes were observed: i) initial increase over first 8 h due to SiO_2 glass formation; ii) rapid loss over period 8–50 h; iii) constant rate loss over period 50–130 h; iv) slow loss above 130 h.	Bubble formation from gases generated at SiC/SiO_2 interface; low viscosity of SiO_2 layer leads to gas escape & formation of holes. Latter act as diffusion channels into C/C matrix.	[33]
Chemical vapour deposition (CVD)	Isothermal 1200 °C for 4 h & 1500 °C for 6 h.	At 1200 °C, 22% mass loss after 4 h. At 1500 °C, 18% mass loss after 6 h.	1200 °C: no obvious SiO_2 was observed, so failure due to diffusion through cracks in SiC. 1500 °C: thin SiO_2 film present but unable to heal surface cracks. Some evidence of CO_2 bubbles under the SiO_2 layer and SiO_2 rods observed, believed to have formed from SiO generated from interfacial reactions.	[15]
CVD (with transition layer between coating and substrate formed by pre-oxidation treatment)	Isothermal 1500 °C for 12 h.	0.5% mass loss after 12 h.	Whilst small microcracks from transition layer caused small CTE mismatch, SiO_2 film could flow and healed smaller cracks.	[34]
Two step CVD and Pack cementation	Continuous TGA to 1500 °C	8.95% mass loss after TGA to 1500 °C.	Coating cracked lead to oxygen diffusing through to C/C composite beneath.	[24]
Coating method not revealed (Manufactured by Lockheed Martin Missiles and Fire Control in Dallas, USA)	Isothermal for 2.5 h at 1000, 1100, 1200 & 1300 °C	1000 °C: Greatest & linear mass loss due to lack of passive SiO_2 layer. 1100 °C, 1200 °C & 1300 °C: Parabolic mass gain then loss due to SiO_2 layer forming. Least loss for the 1300 °C sample.	Linear mass loss due to oxidation through cracks in SiC. Parabolic mass loss due to passive SiO_2 layer forming.	[35]
Halide activated pack cementation (HAPC)	Continuous TGA to 1200 °C with 5, 8, 12 & 15°Cmin^{-1} heating rates	80% mass loss recorded even below 1000 °C.	Activation energy calculations yielded: 59–64 kJ mol^{-1} between 592 – 767 °C 164–184 kJ mol^{-1} between 735 – 938 °C	[13]

environments at elevated temperatures [10]. Many techniques have been developed to deposit a SiC coating onto carbon fibres; the key attribute being the ability to create a dense, homogenous, adherent, defect-free coating that is created throughout the preform, including internally within the carbon fibre tows [11]. Examples of processes include: slurry-sintering [12], pack cementation (PC) [13,14], chemical vapour deposition (CVD) [12,15,16], precursor infiltration and pyrolysis (PIP) [17], sol-gel [18], plasma-enhanced CVD [19] and chemical vapour infiltration (CVI) [20]. PC is one of the most popular techniques and several studies have been conducted to investigate the oxidation resistance of the resulting SiC coating [12,13,15,21–26]. The results indicate that PC-SiC coatings provide excellent oxidation resistance, being able to protect C/C composites from oxidation for more than 310 h at 1500 °C in air [27]; a result that was somewhat better than that for CVD-SiC coatings at elevated temperatures [15] or those formed by slurry-sintering [28–31]. Table 1 summarises some of the literature data on the oxidation behaviour of SiC-coated carbon fibres with the coatings being applied by a range of different coating methods [13,15,24,32–35].

The major limitations of all these SiC coatings, however, are their poor oxidation resistance above about 1500 °C and/or in low oxygen partial pressures and the presence of moisture. Although the rare earth silicates are known to make good environmental barrier coatings, EBCs, for jet engine components, significantly improving the oxidation and corrosion resistance at elevated temperatures [36–39], few studies have considered doping the SiC coatings on carbon fibres with rare earth (RE) oxides.

The advantage of yttrium silicate, Y_2SiO_7, is its low coefficient of thermal expansion (CTE) and low vapour pressure compared to SiO_2 and Y_2O_3 [38,40]. Kang et al. [41] reported that yttrium oxide forms Y^{3+} ions that link with non-bridging oxygen atoms in the SiO_2 structure and consequently result in a more viscous melt [41]. The effect of the transition metals hafnium and zirconium, in terms of their interaction with silica at high temperatures, has also been well reported [42] with the data indicating an improvement in the oxidation resistance by retarding the evaporation of the silica. Hafnia, HfO_2, creates an immiscible phase in silica glass until its reaction with silica to form hafnium silicate, $HfSiO_4$, at higher temperatures. The immiscible phase is reported to increase the viscosity of the glassy silica layer, whilst the $HfSiO_4$ decreases the size of the cracks that form in the silica and hence increases its oxidation protection [42]. Zirconium oxide is also reported to form a silicate, $ZrSiO_4$, which reduces the vaporization of silica [43]. It also has a higher melting point than silica [44] and increases the viscosity of the silica glass via the formation of an immiscible phase, in a similar manner to hafnia. Ceria's interaction with silica is far less well researched; reactions between SiO_2 and CeO_2 have been reported to form $Ce_2Si_2O_7$, $Ce_{4.67}(SiO_4)_3O$ and Ce_2SiO_5 [45].

In the present work, the addition of two rare earth (RE) oxides to SiC-coated carbon fibre preforms has been investigated, for the first time to the authors' knowledge, to improve the oxidation resistance. The two rare earths were yttria, Y_2O_3, and ceria, CeO_2; they were added both separately and in combination. The resulting preforms were subject to temperatures in the range of 1300–1700 °C in dry air with and without the RE oxide dopants being present. The samples were characterised before and after both continuous and isothermal oxidation studies.

2. Experimental procedure

2.1. Sample preparation

2.5D needled PANOX C_f preforms (Surface Transforms, Cheshire, UK) with a fibre volume fraction of about 23% were selected as the starting material with samples measuring 30 mm Φ and being cut from 18 mm thick sheets. These were infiltrated with slurries of rare earth (RE) oxide particles by an injection method. Y_2O_3 (supplier: Alfa Aesar, 99.9% purity, average particle size: 5 μm) or CeO_2 (supplier: Acros Organics, 99.9% purity, average particle size: ≤1 μm) slurries were prepared in a fluid medium of acetone (AR grade, Sigma Aldrich, Dorset, UK) in a vol% ratio of 1 : 5 of RE oxide: acetone. All slurries were ball milled for 48 h in polyurethane lined plastic bottles with alumina media. The slurry was injected directly into the carbon fibre fabrics using 21 gauge needles, bevelled at an angle of 16°. The slurry was injected by plunging the needle to the bottom surface of the preform and then raising it at a

Table 2
Details of samples prepared for different types of oxidation studies.

Sample code	Sample	Vol% CeO_2	Vol% Y_2O_3	SiC coated	Continuous oxidation by TGA	Isothermal oxidation at 1300, 1400 or 1700 °C
RE metal oxides infiltrated into carbon fibre preforms						
CCeY	2.5D Cf + 10 vol% CeO_2+ 10 vol% Y_2O_3	10	0	No	Yes	No
SiC coated carbon fibres with or without infiltrated RE metal oxides						
CS	2.5D C_f	0	0	Yes	Yes	Yes
CCeS	2.5D Cf + 10 vol% CeO_2	10	0	Yes	Yes	Yes
CYS	2.5D C_f + 10 vol% Y_2O_3	0	10	Yes	Yes	Yes
CCeYS	2.5D C_f + 5 vol% CeO_2 + 5 vol% Y_2O_3	5	5	Yes	Yes	Yes
SiO_2 powder mixed with or without RE metal oxides						
S	SiO_2	0	0	No	No	Yes[a]
SCe	SiO_2+ 10 vol% CeO_2	10	0	No	No	Yes[a]
SY	SiO_2+ 10 vol% Y_2O_3	0	10	No	No	Yes[a]
SCeY	SiO_2+ 10 vol% CeO_2+ 10 vol% Y_2O_3	5	5	No	No	Yes[a]

[a] Isothermal heating done at 1700 °C only.

constant speed whilst the plunger was depressed at a constant rate. With a withdrawal speed of 4.5 mm s^{-1} a slurry flow rate of ~0.25 cm^3 s^{-1} was achieved. The injections were made across the whole of the sample in a grid of injection points with the optimum nearest neighbour spacing being found to be 5 mm for the particular preforms and using an outwards spiral injection pattern. This yielded a uniform and homogeneous distribution of slurry throughout the preforms. Further information on the injection technique can be found elsewhere [46].

A total of 10 vol% of CeO_2 or Y_2O_3 particles or a mixture of both was injected into the preforms before the samples were placed in an oven at 125 °C for 12 h to dry. The mass of the samples was recorded before and after injection to ensure the required quantity of RE oxides was added. A 4 mm Φ die punch was used to cut many smaller samples from each of the 30 mm diameter discs before a SiC coating was introduced onto the carbon fibres using conventional isothermal chemical vapour infiltration, CVI (Archer Technicoat Ltd, High Wycombe, UK). The process involved the samples being placed in a specially designed perforated graphite cage to maximize the exposure of the sample to the flowing reactant gases and then methyltrichlorosilane, MTS, gas, catalysed by $H_{2(g)}$, was passed through the samples whilst the latter were heated at 1000 °C for 10 h at 10 Pa. The reaction that occurred is given by:

$$CH_3SiCl_{3(g)} + (n)H_{2(g)} \rightarrow SiC_{(s)} + 3HCl_{(g)} + (n)H_{2(g)} \quad (1)$$

Each sample was weighed before and after the CVI process to determine the mass of the SiC coating deposited and the sample surfaces and cross sections were analysed by XRD (model D8, Bruker, Massachusetts, United States) and SEM-EDS (model TM3030Plus, Hitachi, Tokyo, Japan) to identify the coating phase and thickness at different locations. Also, to confirm the results of what happens to the SiO_2 formed by the oxidation of the SiC coating, direct mixtures of SiO_2 with RE oxides were also heat treated at different temperatures. Details of all samples which were prepared and used for the different tests are summarised in Table 2, with sample codes being provided for ease of identification.

2.2. Oxidation studies

All 4 mm Φ samples were subjected to continuous and isothermal oxidation studies. TGA analysis of all samples was carried out up to 1500 °C in air with a heating rate of 10 °C min^{-1} (model STA 449C, Netzsch, Selb, Germany); 5 mm Φ recrystallized alumina crucibles being used to hold the samples and as a reference. Separate isothermal oxidation studies were conducted at temperatures of 1300, 1400 and 1700 °C in air for up to 6 h in alumina crucibles in a resistance heated furnace. Each sample was weighed before and after heating to determine the mass change during oxidation and the mass loss rate, *Δm%*, was calculated according to Eq. (2):

$$\Delta m\% = \frac{(m1 - m2)}{m1} \times 100 \quad (2)$$

where m1 and m2 were the mass before and after oxidation. Oxidised surfaces were analysed by XRD to identify the phases, whilst the morphology and thickness of the oxide layer were examined by SEM-EDS. Selective oxidised samples were characterised by TEM (2100, JEOL, Tokyo, Japan) with selective area electron diffraction pattern (SAED) and EDS (Oxford Instruments, Oxford, UK). For TEM investigations, a small quantity of ground oxidised sample was added into ethanol solution and the latter exposed to ultrasonic agitation for 10 min. Subsequently a drop of the suspension was placed on a carbon coated copper grid for the analysis; a method often called drop casting.

The oxidation layer growth rate was calculated for all the isothermal oxidation samples at 1300 °C & 1400 °C using the Deal and Grove model [47]:

$$X^2 + AX = B(t + \tau) \quad (3)$$

where X was the oxide thickness in micrometres, t was the time in seconds and A & B were the rate constants. It was assumed that $\tau = 0$ for all equations since this was very small due to it being the growth rate in the thin oxide region [47]. Equation (4) was then used to calculate the growth rate, dx/dt, in μm s^{-1}, the values subsequently being converted to μm h^{-1}.

$$\frac{dx}{dt} = \frac{B}{A + 2X} \quad (4)$$

3. Results

3.1. Starting materials

Fig. 1 shows SEM images of the starting materials. The PANOX carbon fibres, which had an average diameter of ~9 μm, are shown in Fig. 1a whilst Fig. 1b shows the fibres after the injection of the RE oxide particles; the latter are the bright phase. The SiC coating morphology and cross sectional thickness are revealed in Fig. 1c & d; all the carbon fibres throughout the 2.5D C_f preforms were uniformly coated with a crack-free layer of SiC that had an average thickness of 2.17 μm. The lumps in the otherwise smooth SiC coating in Fig. 1d reveal where the RE oxide particles were located beneath the coating. Fig. 2 presents a cross-section of a typical SiC-coated C fibre doped with RE oxide particles and a series of elemental maps.

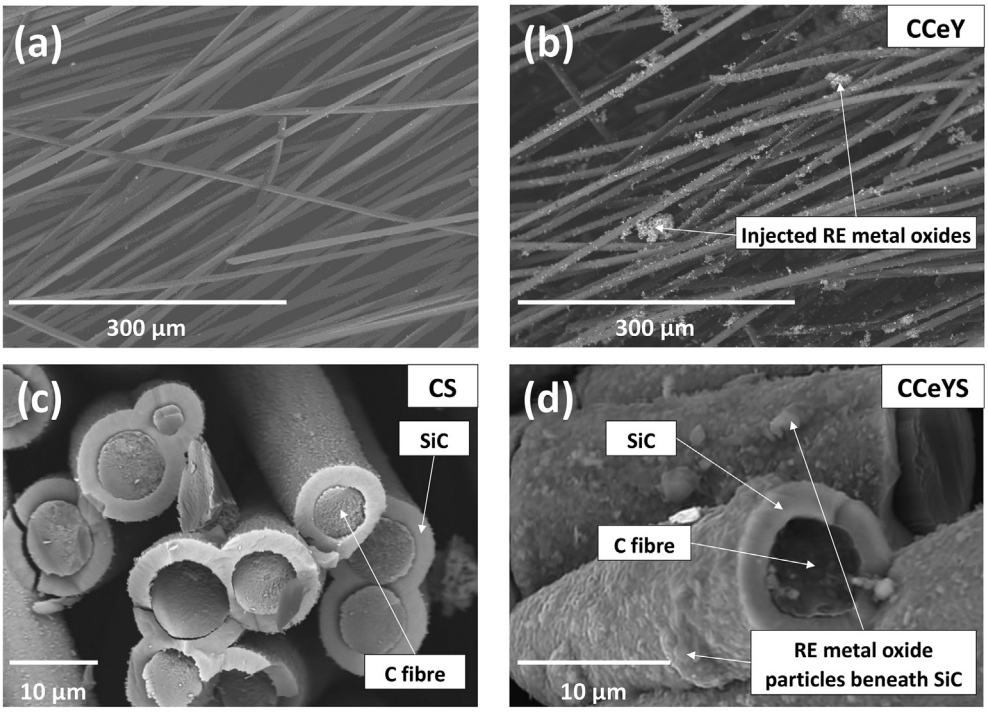

Fig. 1. SEM images of a) 2.5D carbon fibres, b) fibres with RE oxide particles and cross sections of SiC coated on 2.5D C_f c) without and d) with RE oxides.

3.2. Continuous oxidation studies

Fig. 3 shows the plot of mass change vs temperature for the continuous oxidation studies carried out in air using a TGA with a heating rate of 10 °C min^{-1} up to 1500 °C. Although mass loss was observed in all the samples as expected, those without a SiC coating showed a much greater loss even though they still contained the RE oxide particles. Mass loss started at a temperature of ~660 °C, which is typical for the oxidation of carbon fibres. Thus without the SiC coating the RE oxide particles could not protect the carbon fibres from oxidation, presumably due to the lack of formation of a glassy phase. Hence, these samples were not investigated further during the subsequent isothermal oxidation studies.

The curves for the SiC coated samples are shown magnified in the inset of Fig. 3. Weight loss started above ~800 °C with the highest weight loss being recorded in the sample with no rare earth doping; ~11% by 1500 °C. The samples doped with either CeO_2 or Y_2O_3 performed

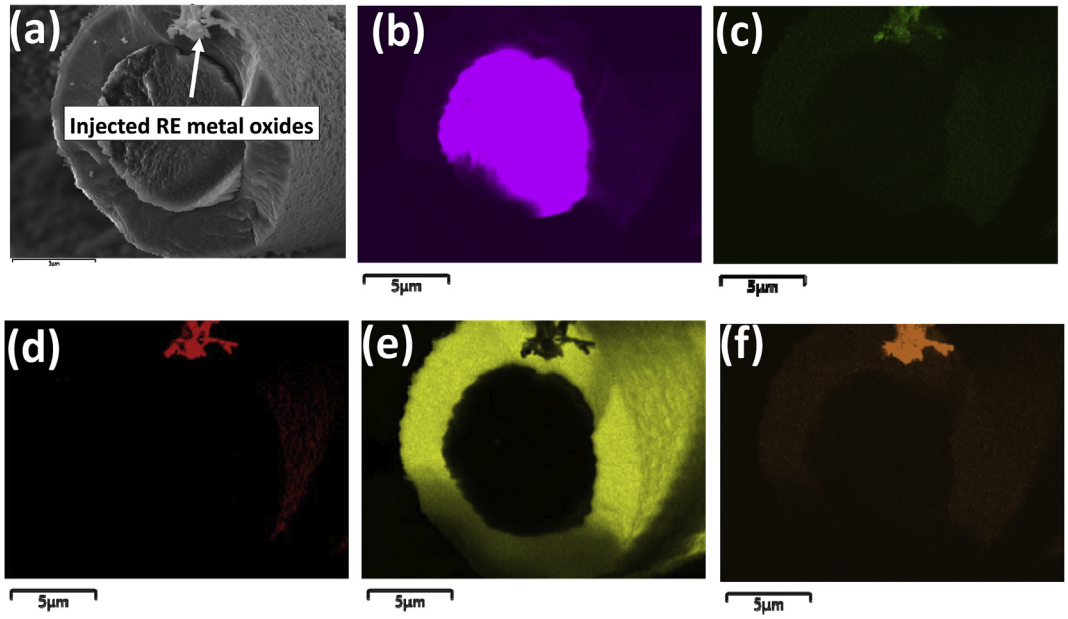

Fig. 2. SEM-EDS image of the sample shown in Fig. 1d showing a) a cross sectional image of the SiC-coated fibre doped with RE oxide particles together with elemental maps of b) C, c) Ce, d) O, e) Si and f) Y.

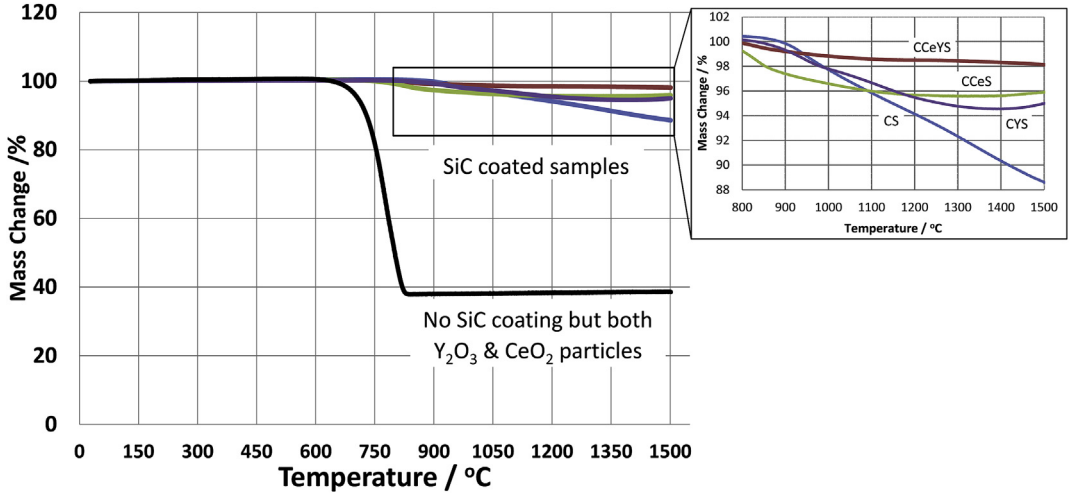

Fig. 3. Results of continuous oxidation by TGA for 2.5D carbon fibre preforms with and without a SiC coating and both undoped and doped with RE oxide particles; see text for heating conditions. The inset shows the SiC coated samples in more detail: CS – no RE oxide particle doping; CYS–Y_2O_3-doped; CCsC–CeO_2-doped; CCeYS–Y_2O_3 & CeO_2-doped.

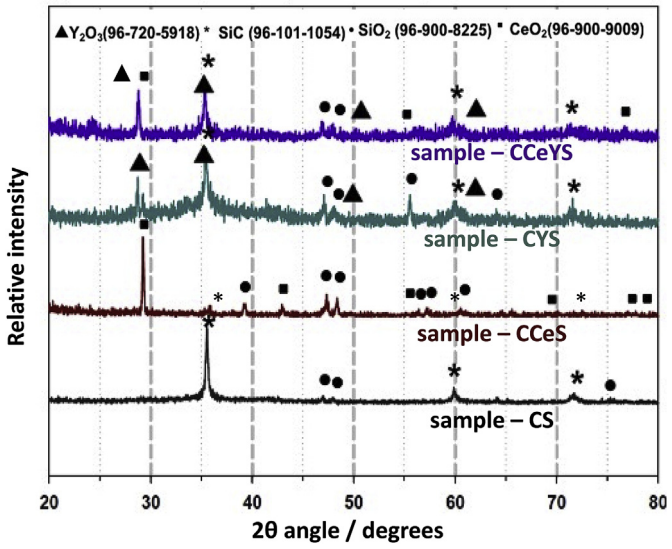

Fig. 4. XRD results for the TGA samples after continuation oxidation in air to 1500 °C. The peaks correspond to the different oxidation products.

similarly; losing ~4 wt% by ~1300 °C and with no further change on additional heating. Interestingly, the Y_2O_3-doped sample appeared to be more protected at lower temperatures, whilst the CeO_2-doped sample was more protected at higher temperatures. The sample with both rare earth oxides only lost ~2 wt% and this occurred steadily up to 1500 °C, the maximum test temperature.

The results of the XRD analysis after the TGA heating are shown in Fig. 4. Note that the sample without the protective SiC coating could not be analysed by XRD due to the very significant mass loss that had occurred. Although tiny peaks of SiO_2 were observed for all the other samples, the dominant peaks were of SiC and the relevant rare earth oxide(s). The XRD patterns show a degree of amorphous nature suggesting the presence of a glassy phase, however this oxide layer must have been thin enough to allow the SiC peaks underneath to be detected.

The SEM images of the oxidised surfaces of the TGA samples are shown in Fig. 5 and confirm the results of the XRD analysis; a thin, continuous and crack free SiO_2 layer can be seen on the surface of all the oxidised fibres. The thicknesses of these layers are recorded in Table 3; they are 0.56 μm for the undoped SiC coated sample, 0.33 & 0.31 μm for the CeO_2 and Y_2O_3 -doped SiC coated samples respectively and just 0.11 μm for the samples containing both the RE oxide particles. It will also be noted that without the latter the carbon fibres have been burnt out leaving hollow SiC tubes, whilst when both the RE oxides dopants were present the carbon fibres remained partially protected.

3.3. Isothermal oxidation studies of SiC coated samples

With respect to the isothermal oxidation studies carried out at 1300, 1400 and 1700 °C for periods up to 6 h in static air, the 1300 and 1400 °C oxidation studies showed no significant difference in mass loss for the undoped and RE-doped SiC coated samples. Fig. 6, however, shows a significant difference for the samples oxidised at 1700 °C. The initial small weight loss observed could be due to the oxidation of the ends of the exposed carbon fibres during the initial ½ h period since after 1 h of oxidation a slight increase in weight was observed for all the samples. A limitation of this study was that cutting the samples during preparation meant the uncoated carbon fibre ends were exposed to oxidation immediately. This has made it difficult to compare mass change data with past studies and also to know whether failures in the SiC coating were a reason for the mass loss. Nevertheless, after this initial period there was little further change of weight for the RE oxide-doped samples, whilst the undoped samples showed a continuous weight loss with increasing exposure time, reaching a maximum weight loss of ~80% after 6 h at 1700 °C; this effectively destroyed the samples.

Fig. 7a and b shows the results of the XRD analysis for the samples isothermally oxidised at 1300 °C and 1400 °C respectively. As for the continuous oxidation XRD results, the primary peaks of both the SiC and the RE oxides can be observed in all the samples, along with some SiO_2 cristobalite peaks. The data from the 1400 °C oxidation samples also shows a greater degree of amorphous nature with fewer peaks from the crystalline phases showing through, particularly for the samples CS, CCeS and CYS, suggesting a thicker silica glass layer was formed. These observations are similar to the XRD results obtained from the TGA samples shown in Fig. 4.

Fig. 8 shows SEM images of the samples with and without the mixed CeO_2 & Y_2O_3 RE-oxide particle doping following 6 h isothermal oxidation holds at 1300, 1400 & 1700 °C. After 1300 °C, Fig. 8a – d, the surfaces are covered with a uniform, adherent, crack-free protective oxide layer and there is some evidence for flow of the glassy silica film. There was relatively little difference between the RE-doped and undoped

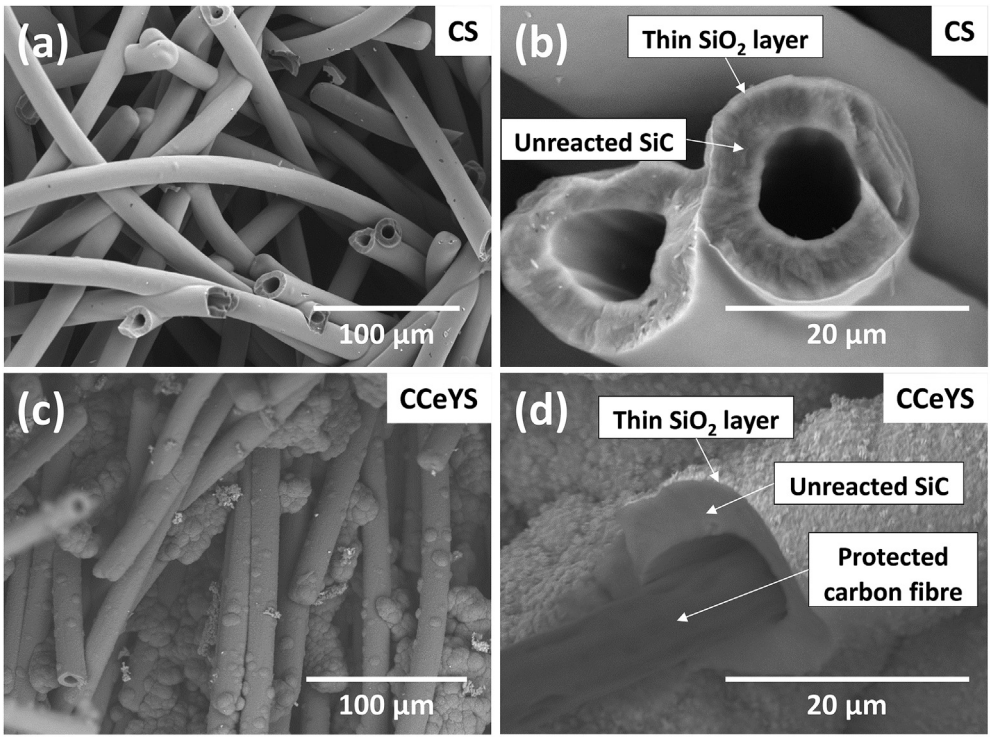

Fig. 5. SEM images of the oxidised samples after TGA, a) & b) the SiC-coated carbon fibres; c) & d) the SiC-coated carbon fibres doped with both CeO_2 & Y_2O_3 particles.

Table 3
Cross sectional oxide layer thickness and growth rate data for oxidised samples as per Deal and Grove model [47].

SiC coated Samples	TGA cont. oxid. to 1500 °C/µm	Isothermal 1300 °C, 30 min /µm	Isothermal 1300 °C, 8 h /µm	Av. growth rate 1300 °C /µm h^{-1}	Isothermal 1400 °C, 30 min /µm	Isothermal 1400 °C, 8 h /µm	Av. growth rate 1400 °C /µm h^{-1}	Isothermal 1700 °C, 30 min /µm
CS	0.56	0.42	1.52	0.364	0.52	0.92	0.091	–
CCeS	0.33	0.14	0.27	0.032	0.28	0.55	0.067	1.84
CYS	0.31	0.36	0.63	0.061	0.16	0.51	0.113	1.90
CCeYS	0.11	0.16	0.26	0.021	0.41	0.48	0.011	1.80

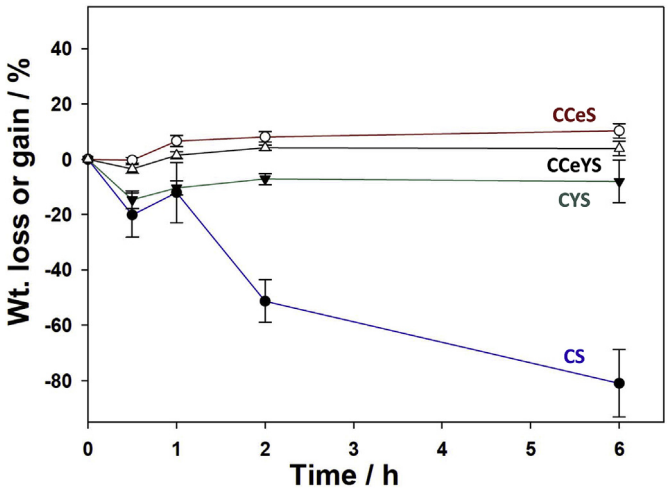

Fig. 6. Mass change vs time plots for the isothermal oxidation studies at 1700 °C in static air for all samples.

samples. After oxidation at 1400 °C, Fig. 8e – h, many of the exposed carbon fibre ends had been sealed by the silica layer that had grown on the exposed carbon fibres of the undoped samples. The higher magnification images show the presence of some cracks that were probably formed due to the difference in thermal expansion coefficients of the surface oxide layer with the SiC coating below it. Apart from the presence of the RE oxide phase, there was once again relatively little difference between the undoped and doped samples. In complete contrast, 6 h of oxidation at 1700 °C completely destroyed the undoped samples, with 80% mass loss occurring; there was so little material left. Fig. 8i – l shows the results for the sample undoped and doped with the RE oxide. Undoped sample shows the glassy phase has spread right across all the fibres due to the low viscosity of the glass at 1700 °C, Fig. 8j, nevertheless carbon fibres still remain, Fig. 8k. Fig. 8l shows the presence of an immiscible secondary phase within the glassy material; EDS spot analysis suggested it was the RE oxide particles that had become trapped. Fig. 9 shows a TEM image of the same region shown in Fig. 8l. The EDS data shows that whilst the Si and O were uniformly distributed as expected, the Y and Ce were present only in the immiscible phase. The selected area electron diffraction pattern, Fig. 9f, however, indicated that the immiscible secondary phase was not the RE oxide particles themselves but the rare earth silicate of $(Ce,Y)_2Si_2O_7$ indicating that the oxide particles had

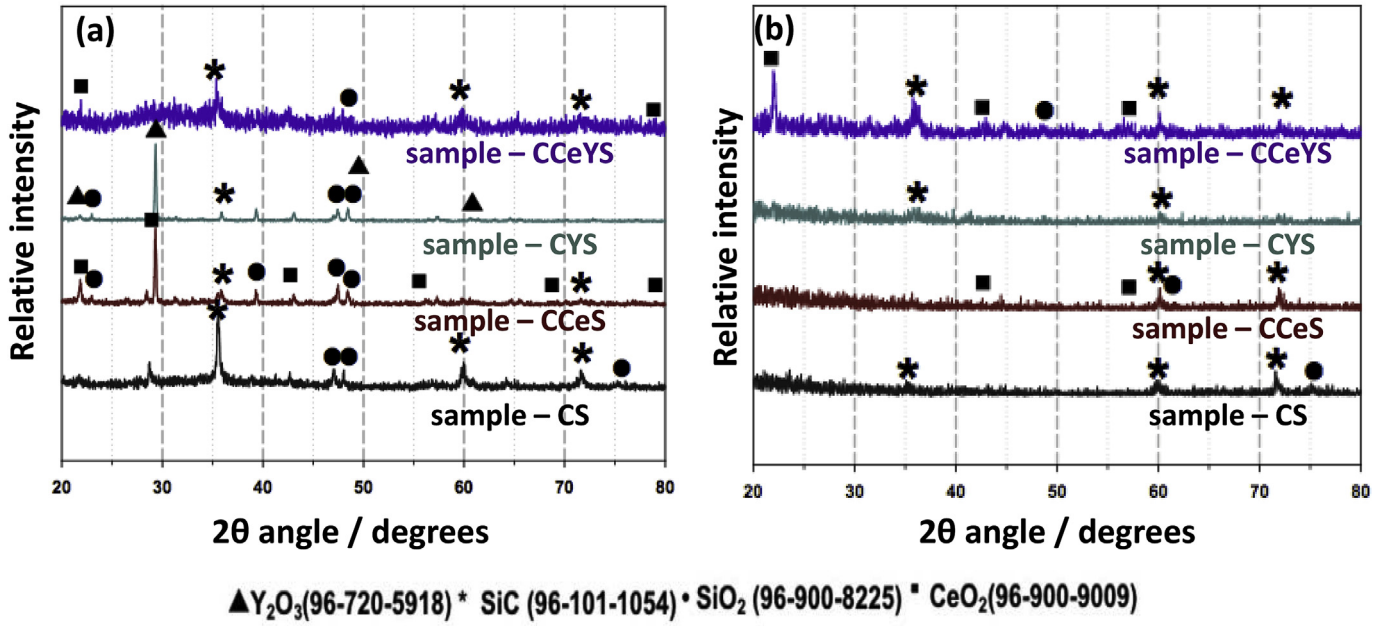

Fig. 7. XRD plots of the isothermal oxidation samples after oxidisation at a) 1300 °C and b) 1400 °C in air. The peaks corresponding to the different constituents are indicated together with their PC-PDF numbers.

reacted with the SiO_2.

Table 3 shows the oxide scale thicknesses developed after the oxidation heat treatments. As expected, higher temperatures and longer times results in thicker oxide layers, whilst the presence of the RE oxides provided increased protection. Oxide growth rates were calculated at 1300 and 1400 °C using the Deal and Grove model [47] and the CeO_2 was observed to provide superior protection at 1300 °C, the Y_2O_3 at 1400 °C and the combination was better at both temperatures and times.

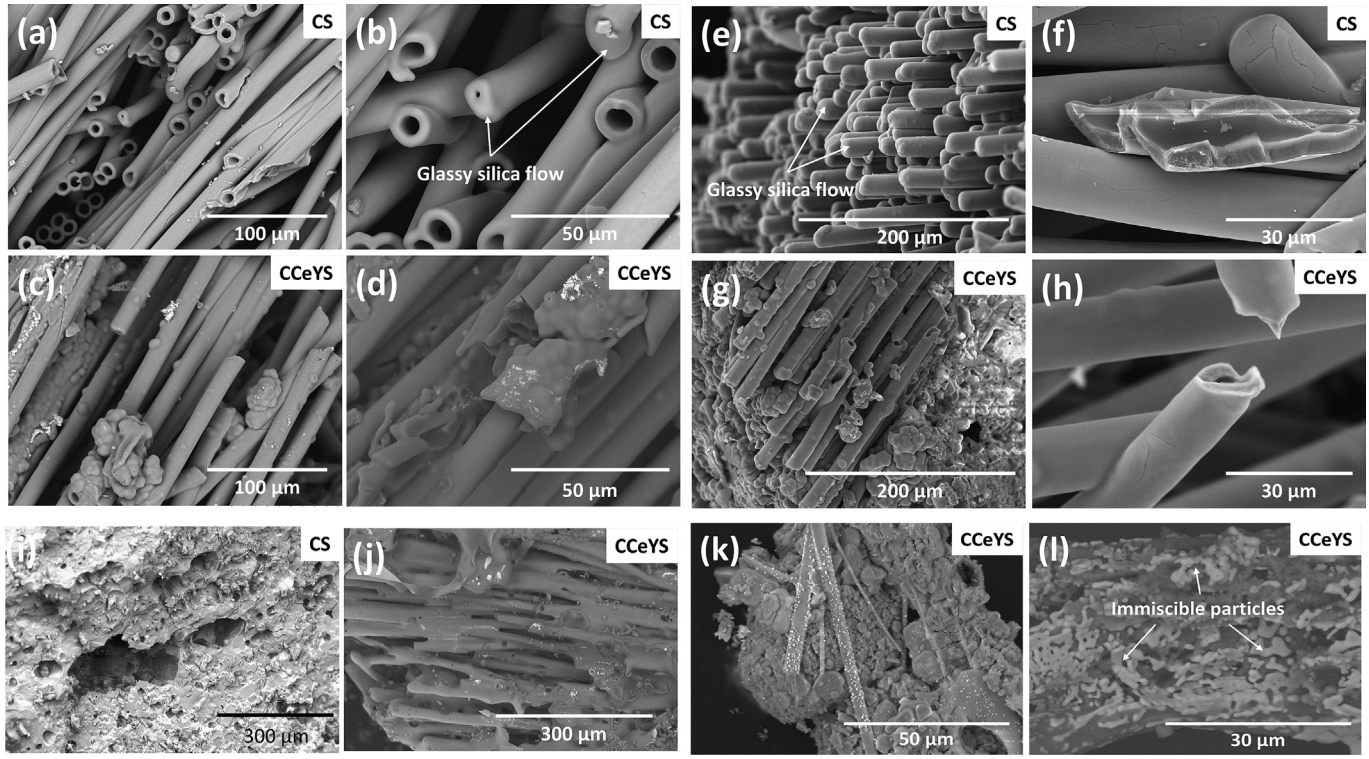

Fig. 8. SEM images of the isothermally oxidised samples after 6 h at: 1300 °C a) & b) undoped, c) & d) doped with both RE oxides; 1400 °C e) & f) undoped, g) & h) doped with both dopants; 1700 °C i) undoped and (j to l) doped with both dopants and different magnifications at different locations.

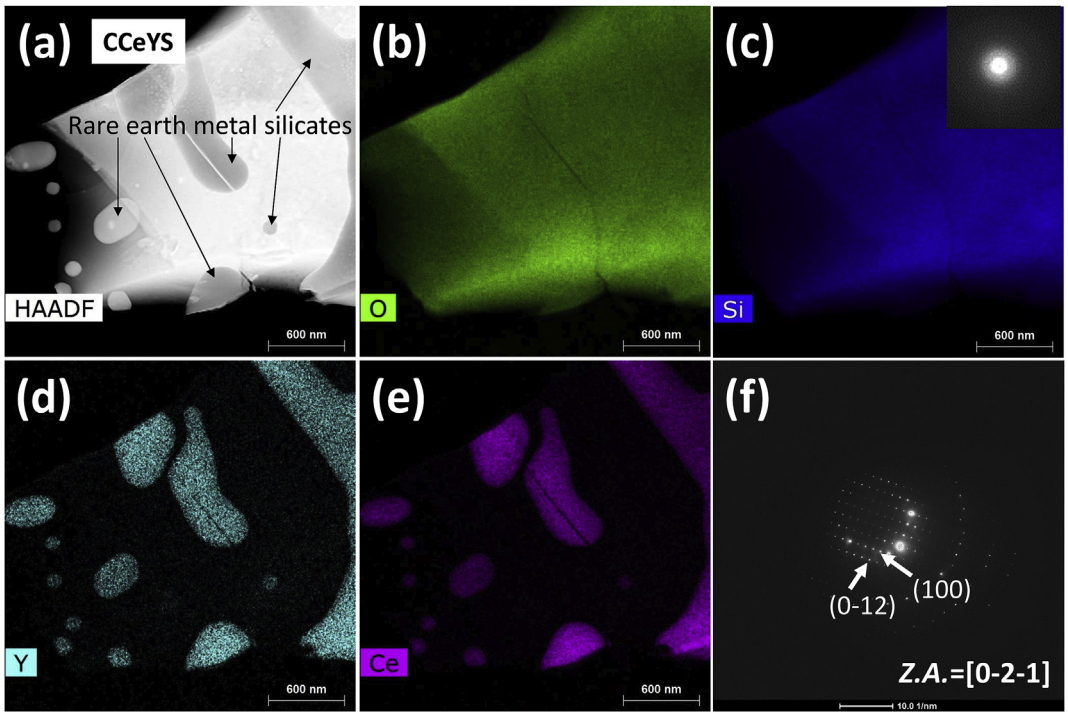

Fig. 9. STEM image of same area shown in Fig. 8l showing a) regions of RE metal silicates trapped in the amorphous SiO_2 layer; elemental maps of b) O, c) Si, d) Y, e) Ce and f) a selected area diffraction pattern (SAED) confirming the crystal structure of the RE oxide silicate. Inset in (C) shows the amorphous SiO_2.

3.4. *High temperature treatment of SiO_2 with and without RE oxide powders*

Fig. 10 shows mass change data for SiO_2 with and without the addition of the RE oxide powders after exposure to 1700 °C for different time intervals. The results are similar to the data in Fig. 6 for the SiC-coated C_f samples. In all cases, there was an initial significant mass loss then the rate of loss decreased substantially. In each case, the presence of the RE oxides reduced the amount of mass loss. Whilst the pure SiO_2 sample lost ~75% of its mass overall after 6 h, the Y_2O_3-doped sample only lost ~30%, the CeO_2-doped sample ~15% and the sample with both RE oxide particles <10%.

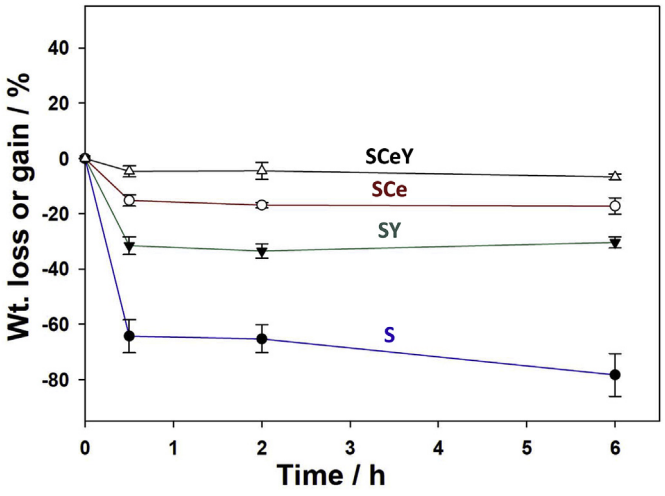

Fig. 10. Mass change vs time plots for the isothermal heating to 1700 °C of SiO_2 with and without the RE oxide particles.

Fig. 11 shows the XRD analysis results after heating the mixtures of SiO_2 with the RE oxide particles for 2 h at 1700 °C. The presence of RE silicates, $Ce_2Si_2O_7$ and $Y_2Si_2O_7$, were observed in these samples, a reaction that is thermodynamically feasible by 1000 °C and has been experimentally demonstrated by Gu et al. [48] and Yang et al. [49] as well as in the current work. The mass loss may be explained by the volatilisation of the SiO_2 at 1700 °C; holes may be seen in the structure in Fig. 12a for the pure SiO_2 whilst they are markedly reduced in number in Fig. 12 b, c & d.

3.5. *Discussion*

The ability of molten silica or silicates to flow at elevated temperature and hence fill and heal cracks is well documented [35,50]. Chu et al. [50] reported an increase in strength of SiC-coated composites due to the self-healing of cracks by molten silica, and, once the silica layer had formed, it also reduced the diffusion of oxygen [10] thus prolonging the life of the material. In the present work, whilst the presence of RE oxides reduced the oxidation of the carbon fibres as expected, they were only really effective when both the SiC coating and the RE oxide particles were present.

Fig. 13 shows a schematic of the proposed oxidation protection mechanism. Essentially, a thin layer of silica was formed from the SiC coating in all cases, as expected. As indicated earlier, the layer thickness was ~0.56 μm for the undoped SiC coated carbon fibres, Table 3, whilst with the RE oxide particles present, the thicknesses ranged from ~0.33 μm with either Y_2O_3 or CeO_2 down to ~0.11 μm with both. These layers were all quite protective at low temperatures such as 1300–1400 °C, however at much higher temperatures such as 1700 °C the pure SiO_2 layer formed without the RE oxide dopants present became far too fluid and could not prevent oxygen diffusing through it, so the composites were completely destroyed. With the RE oxide particles present, especially when both Y_2O_3 and CeO_2 were present, the layer provided some limited protection, even under conditions of 1700 °C for 6 h, a result confirmed by the mass change data in Fig. 6. The latter result was further

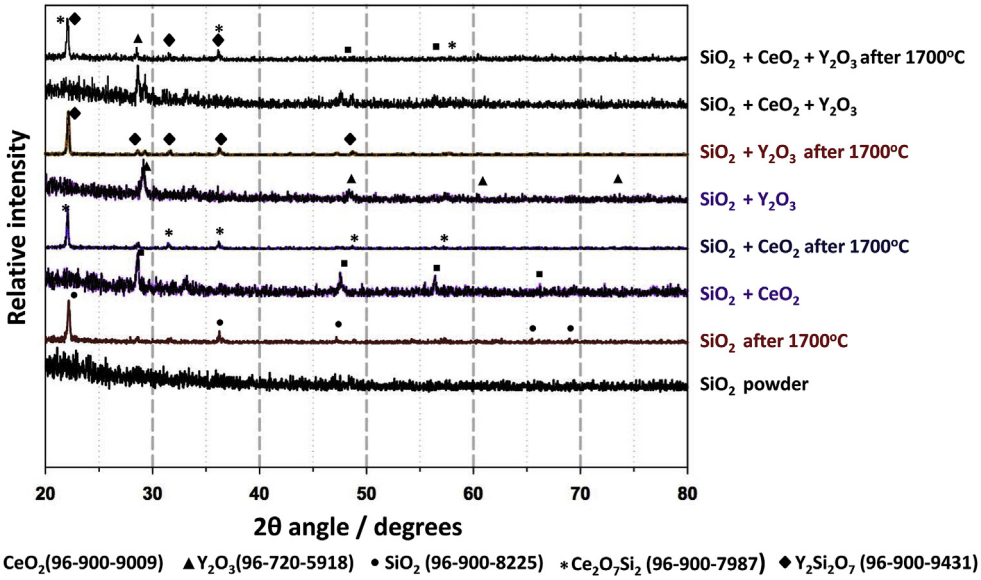

Fig. 11. XRD plots of the SiO_2 with & without RE metal oxide particles before and after heat treatment at 1700 °C for 2 h.

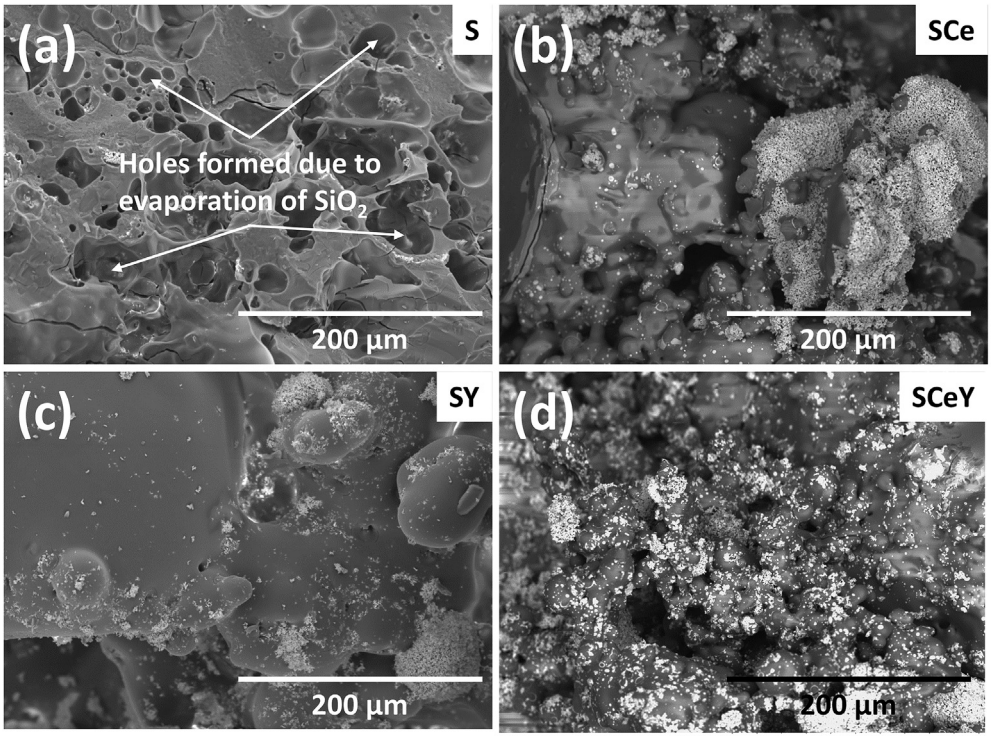

Fig. 12. SEM images of the SiO2 samples exposed at 1700 °C for 1 h with a) no dopant, b) CeO2 particles, c) Y2O3 particles and d) CeO2 & Y2O3 particles.

confirmed by the data in Fig. 10 which showed that when SiO_2 was reacted with Y_2O_3 and/or CeO_2 the resultant silicates formed were less volatile, and hence more resistant to evaporation, and more viscous; similar results have been reported for additions of Yb_2O_3 [51].

$Y_2Si_2O_7$ has been reported previously as having enhanced stability at high temperatures [38] and hence has been used for EBC coatings for high temperature applications. In fact, from RT to 1650 °C, two stable compounds, $Y_2Si_2O_7$ and $Y_2Si_2O_5$, exist in the Y_2O_3–SiO_2 pseudobinary system [52]. The $Y_2Si_2O_7$ forms first, followed by the $Y_2Si_2O_5$ if the Y_2O_3/SiO_2 ratio is ≥ 1. Since only 10 vol% of Y_2O_3 was added, only $Y_2Si_2O_7$ formed in the as-oxidised RE-doped C_f/SiC composite, as confirmed by the XRD patterns shown in Figs. 7 and 11.

Whilst previous work has shown CeO_2 reducing the volatility of B_2O_3 [11], in this work ceria's beneficial effects on reducing silica evaporation

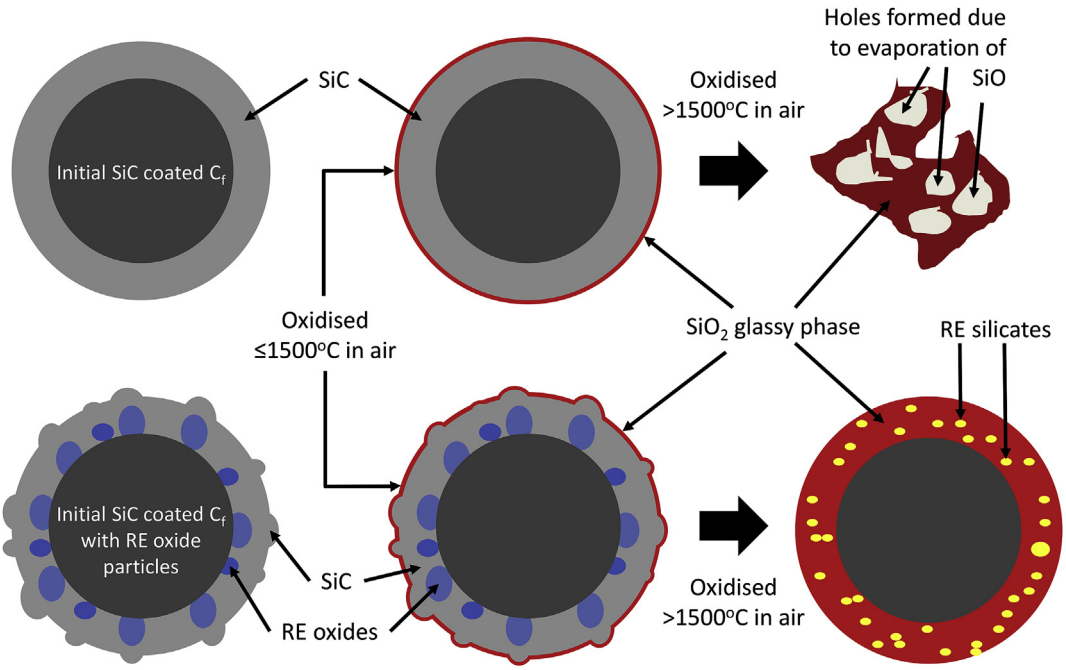

Fig. 13. Schematic outlining the oxidation mechanisms of SiC coated carbon fibres with and without RE oxide particles at different temperatures.

seem to have been superior to yttria's based on the mass loss and oxide growth rate data. This could be due to the finer particle size of the ceria (<1 μm) compared to that of the coarser yttria (~5 μm). However, the combination of the two rare earth oxides yielded particularly good results. In attempting to explain the latter, we need to note that the SiO_2-rich region of the Y_2O_3–SiO_2 phase diagram shows that the addition of small amounts of Y_2O_3 can push the SiO_2 melt into a region containing immiscible liquid phases that are SiO_2-rich and $Y_2Si_2O_7$-rich, respectively. It is well known that such immiscibility between liquid phases can result in an increased viscosity and, as a consequence, both the evaporation of the silica will be suppressed and the oxygen diffusion rate through the liquid layer lowered according to the Stokes-Einstein relationship [53]. However, the formation of these immiscible liquid phases requires a temperature ≥1700 °C. It is possible that the additional of the ceria as well as the yttria might have formed $(Y,Ce)_2Si_2O_7$, which would have a much lower eutectic point compared to the melting temperatures of $Ce_2Si_2O_7$ and $Y_2Si_2O_7$ separately [54]. This, therefore, might explain the superior oxidation resistance in the RE-codoped composites.

Finally, it is worth commenting that the protection was offered by the RE oxide as discrete particles located on the surface of the carbon fibres and under the SiC coating. Previous work has added silicates as a coating in their own right, typically above the SiC coating in the form of an environmental barrier coating (EBC). However, it seems that significant protection can still be achieved without going to this trouble; if true then it should also mean that there will be less layers required and less need to engineer their thermal expansion coefficients, which should result in much easier, and hence cheaper, manufacture of both carbon and silicon carbide fibre composites.

4. Conclusions

This study has reported the oxidation behaviour of SiC coated 2.5D carbon fibre preforms with and without the addition of RE oxides. Important findings are that the CVI method allows the production of dense, homogenous, continuous and defect-free SiC coatings on 2.5D carbon fibres at temperatures as low as 1000 °C. The SiC coating protected the carbon fibres from the oxidizing environment at temperatures up to 1500 °C by the formation of a continuous, crack-free and adherent SiO_2 oxide layer. Any carbon fibres in the preform that had remained uncoated were also protected from oxidation by the spreading of the glassy SiO_2 layer over them. Doping the SiC coating with rare earth oxides of yttria and/or ceria improved the oxidation resistance provided by the coating via the formation of rare earth silicates. The rare earth oxide doping also helped to reduce the growth rate of the oxide layer by reducing the silica volatility and increasing its viscosity. Based on the literature [51], it is believe that this occurred as a result of the RE cations occupying the interstitials without degrading the Si–O bonds of the SiO_2 network and hence the molecular oxygen diffusion rate was decreased. Finally, ceria's beneficial effects on reducing silica evaporation seem to have been superior to yttria's. The combination of the two rare earth oxides yielded particularly good results.

Declaration of competing interest

The authors declare that they have no known competing financial interests or personal relationships that could have appeared to influence the work reported in this paper.

Acknowledgement

This project has received funding from the European Union's Horizon 2020 research and innovation programme under the Marie Sklodowska-Curie grant (EREMOZ) agreement No 748568. The authors would like to acknowledge Mr Frank Biddlestone and Mr Grant Holt for their help with obtaining the TGA and isothermal oxidation data respectively.

References

[1] J. Binner, et al., Selection, processing, properties and applications of ultra-high temperature ceramic matrix composites, UHTCMCs – a review, Int. Mater. Rev. (2019), https://doi.org/10.1080/09506608.2019.1652006. Accepted, no. In Press.
[2] A. Paul, V. Rubio, J. Binner, B. Vaidhyanathan, A. Heaton, P. Brown, Evaluation of the high temperature performance of HfB_2 UHTC particulate filled C_f/C composites,

Int. J. Appl. Ceram. Technol. 14 (3) (May 2017) 344–353, https://doi.org/10.1111/ijac.12659.
[3] A. Paul, S. Venugopal, J.G.P. Binner, B. Vaidhyanathan, A.C.J. Heaton, P.M. Brown, "UHTC–carbon fibre composites: preparation, oxyacetylene torch testing and characterisation, J. Eur. Ceram. Soc. 33 (2) (Feb. 2013) 423–432, https://doi.org/10.1016/j.jeurceramsoc.2012.08.018.
[4] J.K. Sonber, T.S.R.C. Murthy, C. Subramanian, S. Kumar, R.K. Fotedar, A.K. Suri, Investigations on synthesis of ZrB_2 and development of new composites with HfB_2 and $TiSi_2$, Int. J. Refract. Metals Hard Mater. 29 (1) (Jan. 2011) 21–30, https://doi.org/10.1016/j.ijrmhm.2010.06.007.
[5] J.K. Sonber, "Effect of NdB_6 addition on densification and properties of ZrB_2, Ceram. - Silikaty 60 (1) (Mar. 2016) 41–47, https://doi.org/10.13168/cs.2016.0006.
[6] T.S.R.C. Murthy, J.K. Sonber, K. Sairam, S. Majumdar, V. Kain, Boron-based ceramics and composites for nuclear and space applications: synthesis and consolidation, in: Handbook Of Advanced Ceramics And Composites, Springer International Publishing, 2019, pp. 1–36.
[7] T.S.R.C. Murthy, J.K. Sonber, K. Sairam, R.D. Bedse, J.K. Chakarvartty, Development of refractory and rare earth metal borides & carbides for high temperature applications, Mater. Today Proc. 3 (9) (2016) 3104–3113, https://doi.org/10.1016/j.matpr.2016.09.026.
[8] Y. Arai, R. Inoue, K. Goto, Y. Kogo, Carbon fiber reinforced ultra-high temperature ceramic matrix composites: a review, Ceram. Int. 45 (12) (Aug. 2019) 14481–14489, https://doi.org/10.1016/j.ceramint.2019.05.065.
[9] V. Rubio, J. Binner, A. T Ackerman, S. Cousinet, N. Pommepuy, X. Bertrand, Ultra high temperature ceramic composite materials [Online]. Available, https://dc.engconfintl.org/uhtc_iv/52, Sep. 2017. (Accessed 20 May 2019).
[10] J. Roy, S. Chandra, S. Das, S. Maitra, Oxidation behaviour of silicon carbide - a review, Rev. Adv. Mater. Sci. 38 (2014) 29–39.
[11] M.E. Westwood, J.D. Webster, R.J. Day, F.H. Hayes, R. Taylor, Review Oxidation protection for carbon fibre composites, J. Mater. Sci. 31 (6) (1996) 1389–1397, https://doi.org/10.1007/BF00357844.
[12] R. Aliasgarian, M. Naderi, S.E. Mirsalehi, S. Safi, The ablation and oxidation behaviors of SiC coatings on graphite prepared by slurry sintering and pack cementation, J. Mater. Eng. Perform. 27 (8) (Aug. 2018) 3900–3910, https://doi.org/10.1007/s11665-018-3462-z.
[13] J. Prakash, M. Gade, B. Paul, K. Dasgupta, A facile route for graded conversion of carbon fabric to silicon carbide fabric and its oxidation kinetics study in atmospheric high-temperature environment, Bull. Mater. Sci. 41 (108) (Aug. 2018) 1–6, https://doi.org/10.1007/s12034-018-1627-x.
[14] M.H. Hu, K.Z. Li, H.J. Li, B. Wang, H.L. Ma, "Double layer $ZrSi_2$ –ZrC–SiC/SiC oxidation protective coating for carbon/carbon composites, Surf. Eng. 31 (5) (Apr. 2015) 335–341, https://doi.org/10.1179/1743294414Y.0000000428.
[15] L. Li, et al., Comparison of the oxidation behaviors of SiC coatings on C/C composites prepared by pack cementation and chemical vapor deposition, Surf. Coating. Technol. 302 (Sep. 2016) 56–64, https://doi.org/10.1016/j.surfcoat.2016.05.071.
[16] J.Y. Jing, Q.G. Fu, R.M. Yuan, Nanowire-toughened CVD-SiC coating for C/C composites with surface pre-oxidation, Surf. Eng. 34 (1) (Jan. 2018) 47–53, https://doi.org/10.1080/02670844.2017.1292705.
[17] D. Tong, H. Wang, L. Wang, L. Chen, Z. Li, Coating of poly (carborane-carbosilane-phenylacetylene) on carbon fibers with excellent oxidation protection, Surf. Coating. Technol. 319 (Jun. 2017) 335–344, https://doi.org/10.1016/j.surfcoat.2017.04.014.
[18] K. Xia, C. Lu, Y. Yang, Improving the oxidation resistance of carbon fibers using silicon oxycarbide coatings, N. Carbon Mater. 30 (3) (Jun. 2015) 236–243, https://doi.org/10.1016/S1872-5805(15)60188-3.
[19] R. Pillai, N. Batra, L.M. Manocha, N. Machinewala, Deposition of silicon carbide interface coating on carbon fibre by PECVD for advanced composites, Surfaces and Interfaces 7 (Jun. 2017) 113–115, https://doi.org/10.1016/j.surfin.2017.03.006.
[20] R. Naslain, F. Langlais, R. Fedou, The cvi-processing of ceramic matrix composites, J. Phys. Colloq. 50 (C5) (May 1989) 191–207, https://doi.org/10.1051/jphyscol:1989526.
[21] C. Sun, H. Li, Q. Fu, J. Zhang, H. Peng, Double SiC coating on carbon/carbon composites against oxidation by a two-step method, Trans. Nonferrous Metals Soc. China 23 (7) (Jul. 2013) 2107–2112, https://doi.org/10.1016/S1003-6326(13)62703-X.
[22] H. Jian Feng, Z. Xie Rong, L. He Jun, X. Xin Bo, F. Ye wei, Influence of the preparation temperature on the phase, microstructure and anti-oxidation property of a SiC coating for C/C composites, Carbon N. Y. 42 (8–9) (2004) 1517–1521, https://doi.org/10.1016/j.carbon.2004.01.066.
[23] M. Hu, K. Li, H. Li, T. Feng, L. Li, Influence of β-SiC on the microstructures and thermal properties of SiC coatings for C/C composites, Surf. Coating. Technol. 304 (Oct. 2016) 188–194, https://doi.org/10.1016/j.surfcoat.2016.07.010.
[24] Y. Chu, Q. Fu, H. Li, K. Li, X. Zou, C. Gu, Influence of SiC nanowires on the properties of SiC coating for C/C composites between room temperature and 1500°C, Corrosion Sci. 53 (9) (Sep. 2011) 3048–3053, https://doi.org/10.1016/j.corsci.2011.05.046.
[25] H. Li, Y. Wang, Q. Fu, G. Sun, Improvement in oxidation properties of SiC-coated carbon/carbon composites through modification of the SiC/carbon interface, Surf. Coating. Technol. 245 (Apr. 2014) 49–54, https://doi.org/10.1016/j.surfcoat.2014.02.036.
[26] X. Qiang, H. Li, Y. Zhang, D. Yao, L. Guo, J. Wei, Fabrication and thermal shock resistance of in situ SiC nanowire-SiC/SiC coating for carbon/carbon composites, Corrosion Sci. 59 (Jun. 2012) 343–347, https://doi.org/10.1016/j.corsci.2012.01.035.
[27] Q. Fu, H. Li, X. Shi, K. Li, G. Sun, Silicon carbide coating to protect carbon/carbon composites against oxidation, Scripta Mater. 52 (9) (May 2005) 923–927, https://doi.org/10.1016/j.scriptamat.2004.12.029.
[28] Q. Zhu, X. Qiu, C. Ma, Oxidation resistant SiC coating for graphite materials, Carbon N. Y. 37 (9) (1999) 1475–1484, https://doi.org/10.1016/S0008-6223(99)00010-X.
[29] Z. Liu, Q. Guo, L. Liu, J. Shi, G. Zhai, Effect of sintering temperature on microstructure and properties of SiC coatings for carbon materials, Surf. Coating. Technol. 202 (13) (Mar. 2008) 3094–3099, https://doi.org/10.1016/j.surfcoat.2007.11.014.
[30] J. Zhao, L. Liu, Q. Guo, J. Shi, G. Zhai, "Oxidation protective behavior of SiC/Si–$MoSi_2$ coating for different graphite matrix, Mater. Lett. 60 (16) (Jul. 2006) 1964–1967, https://doi.org/10.1016/j.matlet.2005.12.072.
[31] T.M. Wu, W.C. Wei, S.E. Hsu, The effect of boron additive on the oxidation resistance of SiC-protected graphite, Ceram. Int. 18 (3) (Jan. 1992) 167–172, https://doi.org/10.1016/0272-8842(92)90091-Q.
[32] W. Zhou, P. Xiao, W. Luo, Y. Li, Microstructural evolution of SiC coating on C/C composites exposed to 1500 °C in ambient air, Ceram. Int. 45 (1) (Jan. 2019) 854–860, https://doi.org/10.1016/j.ceramint.2018.09.255.
[33] Q. Fu, H. Li, X. Shi, K. Li, G. Sun, Silicon carbide coating to protect carbon/carbon composites against oxidation, Scripta Mater. 52 (9) (May 2005) 923–927, https://doi.org/10.1016/j.scriptamat.2004.12.029.
[34] Y.C. Shan, et al., Improvement of the bonding strength and the oxidation resistance of SiC coating on C/C composites by pre-oxidation treatment, Surf. Coating. Technol. 253 (Aug. 2014) 234–240, https://doi.org/10.1016/J.SURFCOAT.2014.05.042.
[35] N.S. Jacobson, D.J. Roth, R.W. Rauser, J.D. Cawley, D.M. Curry, Oxidation through coating cracks of SiC-protected carbon/carbon, Surf. Coating. Technol. 203 (3–4) (Nov. 2008) 372–383, https://doi.org/10.1016/j.surfcoat.2008.09.013.
[36] D. Zhu, S. Diego, Environmental barrier coatings for turbine engines: current status and future directions the international conference on metallurgical coatings and thin films (ICMCTF) [Online]. Available, https://ntrs.nasa.gov/search.jsp?R=20150009532, 2013. (Accessed 6 May 2019).
[37] Y. Xu, X. Hu, F. Xu, K. Li, Rare earth silicate environmental barrier coatings: present status and prospective, Ceram. Int. 43 (8) (Jun. 2017) 5847–5855, https://doi.org/10.1016/j.ceramint.2017.01.153.
[38] H.J. Seifert, et al., Yttrium silicate coatings on chemical vapor deposition-SiC-precoated C/C-SiC: thermodynamic assessment and high-temperature investigation, J. Am. Ceram. Soc. 88 (2) (Feb. 2005) 424–430, https://doi.org/10.1111/j.1551-2916.2005.00077.x.
[39] X.Q. Feng, et al., Oxidation resistance improvement of ZrB_2 powders by the deposition of $Al_2O_3/Y_2O_3/ZrO_2$ coatings via chemical coprecipitation method, IOP Conf. Ser. Mater. Sci. Eng. 474 (Feb. 2019), 012048, https://doi.org/10.1088/1757-899X/474/1/012048.
[40] E. Courcot, F. Rebillat, F. Teyssandier, C. Louchet-Pouillerie, "Thermochemical stability of the Y_2O_3–SiO_2 system, J. Eur. Ceram. Soc. 30 (4) (Mar. 2010) 905–910, https://doi.org/10.1016/j.jeurceramsoc.2009.09.007.
[41] J. Kang, et al., Effect of Y_2O_3 content on the crystallization behaviors and physical properties of glasses based on MgO-Al_2O_3 -SiO_2 system, J. Non-Cryst. Solids 497 (Oct. 2018) 12–18, https://doi.org/10.1016/j.jnoncrysol.2018.05.029.
[42] P. Wang, H. Li, X. Ren, R. Yuan, X. Hou, Y. Zhang, HfB_2-SiC-$MoSi_2$ oxidation resistance coating fabricated through in-situ synthesis for SiC coated C/C composites, J. Alloys Compd. 722 (2017) 69–76, https://doi.org/10.1016/j.jallcom.2017.06.008.
[43] W.Z. Zhang, Y. Zeng, L. Gbologah, X. Xiong, B.Y. Huang, Preparation and oxidation property of ZrB_2-$MoSi_2$/SiC coating on carbon/carbon composites, Trans. Nonferrous Metals Soc. China 21 (7) (Jul. 2011) 1538–1544, https://doi.org/10.1016/S1003-6326(11)60893-5.
[44] L. Li, et al., Oxidation behavior and microstructure evolution of SiC-ZrB_2 -ZrC coating for C/C composites at 1673 K, Ceram. Int. 42 (11) (Aug. 2016) 13041–13046, https://doi.org/10.1016/j.ceramint.2016.05.083.
[45] S. Zec, S. Boskovic, Cerium silicates formation from mechanically activated oxide mixtures, J. Mater. Sci. 39 (16/17) (Aug. 2004) 5283–5286, https://doi.org/10.1023/B:JMSC.0000039229.35551.9e.
[46] B. Baker, et al., Development of a slurry injection technique for continuous fibre ultra-high temperature ceramic matrix composites, J. Eur. Ceram. Soc. 39 (14) (Nov. 2019) 3927–3937, https://doi.org/10.1016/j.jeurceramsoc.2019.05.070.
[47] B.E. Deal, A.S. Grove, General relationship for the thermal oxidation of silicon, J. Appl. Phys. 36 (12) (Dec. 1965) 3770–3778, https://doi.org/10.1063/1.1713945.
[48] H. Gu, X. Hou, R. Zhang, D. Fang, Novel high - temperature - resistant Y_2SiO_5 aerogel with ultralow thermal conductivity, Int. J. Appl. Ceram. Technol. 16 (6) (Nov. 2019) 2393–2397, https://doi.org/10.1111/ijac.13258.
[49] M. Yang, B. Dong, F. Wang, X. Xu, S. Agathopoulos, Fabrication of α - Si3N4 -nanowire/γ -$Y_2Si_2O_7$ composite superhydrophobic membrane for membrane distillation, Int. J. Appl. Ceram. Technol. 16 (6) (Nov. 2019) 2173–2180, https://doi.org/10.1111/ijac.13247.

[50] M.C. Chu, S.J. Cho, Y.C. Lee, H.M. Park, D.Y. Yoon, Crack healing in silicon carbide, J. Am. Ceram. Soc. 87 (3) (Mar. 2004) 490–492, https://doi.org/10.1111/j.1551-2916.2004.00490.x.

[51] X. Pan, et al., Ablation resistance and mechanism of ZrC-SiC-Yb_2O_3 ternary composite coatings fabricated by vacuum plasma spray, J. Eur. Ceram. Soc. 39 (13) (Oct. 2019) 3604–3612, https://doi.org/10.1016/j.jeurceramsoc.2019.04.041.

[52] I.A. Toropov, N.A. Bondar, Silicates of the rare earth elements, Russ. Chem. Bull. 10 (1961) 502–508, https://doi.org/10.1007/BF00909109.

[53] M.M. Opeka, I.G. Talmy, J.A. Zaykoski, Oxidation-based materials selection for 2000°C + hypersonic aerosurfaces: theoretical considerations and historical experience, J. Mater. Sci. 39 (19) (Oct. 2004) 5887–5904, https://doi.org/10.1023/B:JMSC.0000041686.21788.77.

[54] L.N.S.N.A. Toropov, I.F. Andreev, A.N. Sokolov, Inorg. Mater. USSR 6 (3) (1970) 455.